Characterization of surface water storage changes in Arctic lakes using simulated SWOT measurements

Hyongki Lee[ab]; Michael Durand[b]; Hahn Chul Jung[ab]; Doug Alsdorf[ab]; C. K. Shum[ab]; Yongwei Sheng[c]
[a] Division of Geodetic Science, School of Earth Sciences, The Ohio State University, Columbus, OH, USA [b] Byrd Polar Research Center, The Ohio State University, Columbus, OH, USA [c] Department of Geography, University of California, Los Angeles, CA, USA

Online publication date: 04 August 2010

PLEASE SCROLL DOWN FOR ARTICLE

Taylor & Francis
Taylor & Francis Group

Characterization of surface water storage changes in Arctic lakes using simulated SWOT measurements

HYONGKI LEE*†‡, MICHAEL DURAND‡, HAHN CHUL JUNG†‡,
DOUG ALSDORF†‡, C. K. SHUM†‡ and YONGWEI SHENG§

†Division of Geodetic Science, School of Earth Sciences, The Ohio State University,
275 Mendenhall Laboratory, 125 South Oval Mall, Columbus, OH 43210, USA
‡Byrd Polar Research Center, The Ohio State University, 1090 Carmack Road,
Columbus, OH, 43210 USA
§Department of Geography, University of California, 1255 Bunche Hall, Los Angeles,
CA, 90095, USA

The planned Surface Water and Ocean Topography (SWOT) satellite mission will measure freshwater storage changes in global lakes. Herein, the anticipated SWOT storage change accuracy is evaluated for the lakes in the Peace-Athabasca Delta, Northern Alaska and Western Siberia. Because of the significant lack of Arctic lake measurements, we simulated realistic daily to seasonal changes in water elevations in the study region using a combination of data from lake gauges, satellite radar altimeter, and satellite imagery. This 'truth' dataset is sampled with several candidate SWOT orbits and then corrupted with expected instrument errors to simulate SWOT observed storage changes. The number of revisits increases with increasing or decreasing latitude for a given repeat cycle (e.g. four to eight revisits for a 22-day cycle), allowing us to investigate storage change errors at monthly sampling. SWOT storage change accuracy is primarily controlled by lake size. Lakes larger than 1 km^2 have relative errors generally less than 5% whereas one-hectare size lakes are about 20%. We concluded that the storage change accuracy is insensitive to the orbital inclination or repeat periods, but is sensitive to lake shapes.

1. Introduction

As a readily accessible water resource, lakes house more than 95% of the liquid surface freshwater on the Earth's surface, supporting domestic, agricultural and industrial water supplies (Wetzel 1992). In addition, lakes provide habitat for complex aquatic ecosystems, as well as significant sources of food and aquatic biodiversity. The extent of physical changes to lakes around the world has increased over the past century. Changes in surface water in response to accelerated climate and environmental changes affect the local heat balance and the evaporation rate (Carpenter *et al.* 1992). Hence, the global distribution and changes in lakes are of key social and economic importance.

It is estimated that approximately 2.1% of the terrestrial surface is covered by lakes and ponds exceeding one hectare (Meybeck 1995). Recent work by Downing *et al.* (2006) extrapolated power law-based relationships to develop an estimate that there are over 300 million lakes globally with an area of 0.1 hectare or larger. Despite these pioneering studies, it remains uncertain how many water bodies there are on the surface of the Earth, and what areal fraction of the surface is covered by lakes.

---

*Corresponding author. Email: lee.2444@osu.edu

Estimates of lake water elevations, their volumes and storage changes are even more uncertain. No single comprehensive and systematic high-resolution database of lake distributions is currently available at the global scale. Due to this deficiency, lakes have not been analysed or monitored in detail globally.

Therefore, there is significant uncertainty associated with interseasonal and inter-annual lake dynamics, although surface water storage change is a key term in the water balance at any scale. For instance, Smith *et al.* (2005) noted a marked decrease in the abundance of Siberian lakes between 1973 and 1997; this was attributed to increased temperature, which resulted in the melting of the underlying permafrost, thus allowing the water to evacuate into the groundwater system. Due in part to the concentration of most lakes at high latitudes (Lehner and Döll 2004), lake elevation dynamics are measured *in situ* or via radar altimeter at only a small number of lakes globally. Simultaneous monitoring of water elevation and inundated area (e.g. Smith and Pavelsky 2009) to obtain storage changes is even less common. Therefore, important questions remain unanswered. For example, it is unknown what part of the total interseasonal and interannual variation in terrestrial water storage is attri-butable to lakes, as contrasted with, for instance, soil moisture, ephemeral snow cover or groundwater.

The Surface Water and Ocean Topography (SWOT) mission is a swath mapping radar interferometer that will provide simultaneous measurements of water elevation and inundated area for inland water bodies. SWOT measurements will thus enable the first global characterization of freshwater storage changes, providing the means to address the open science questions mentioned above. SWOT has been recommended by the National Research Council (NRC) decadal survey (NRC 2007) to measure ocean topography as well as water elevations over rivers, lakes and wetlands. The proposed launch of SWOT recommended by the NRC is between 2013–2016. Average revisit times will depend upon latitude, with two to four revisits at low to mid latitudes and up to 10 revisits at high latitudes for a 22-day exact repeat period orbit. In contrast with traditional radar altimeters, SWOT will directly measure fluvial inun-dated area as well as water elevation, with spatial samplings in the order of tens of metres. For the purpose of monitoring surface water storage variations in lakes, reservoirs or wetlands, the key measurements retrieved by SWOT will be repeat observations of surface water elevation and inundated area, from which storage change can be readily calculated. These will provide systematic and comprehensive assessments of natural and human-induced lake dynamics at regional and global scales. However, no studies have yet examined the expected accuracy of lake storage changes using SWOT. Of special interest is to quantify SWOT storage change accu-racy as a function of lake size. This paper aims to study the level of fidelity that SWOT storage change data is expected to achieve, and the extent to which SWOT measure-ments will be able to provide information on terrestrial storage change for millions of lakes that are currently unmeasured.

Specifically, the main objectives of our paper are (1) to quantify the expected accuracy of storage change data from SWOT for lakes in three high-latitude study areas (§2.1); and (2) to evaluate the sensitivity of SWOT accuracy to the choice of SWOT orbital parameters, including the orbital inclination and exact repeat orbit periods. We will accomplish these objectives within the context of a SWOT 'virtual mission', in which we (1) simulate a realistic estimate of 'true' variations in lake water elevations, inundated areas, and storage changes; (2) generate 'truth' SWOT observa-tions by performing spatiotemporal sampling of the truth water elevations (§2.3) and

inundated areas (§2.4), and by corrupting the simulated observations with expected SWOT measurement errors; (3) using the corrupted SWOT observations to recreate the truth (§2.5), and (4) comparing the true and SWOT-derived storage change estimates (§3).

2. Methods and data

2.1 *Study areas*

Our three study areas include the Peace–Athabasca Delta (PAD) in Canada, and the Northern Alaskan and West Siberian Arctic regions. These three regions represent high-latitude geographies where most global lakes are distributed (see figure 2 of Lehner and Döll (2004)). Indeed, the highest concentration of the lakes is found between $50°$ N and $70°$ N. PAD is among the world's largest and most ecologically significant inland fresh water deltas. It is characterized by low relief and high complexity, consisting of hundreds of shallow lakes, wetlands and distributary channels with varying degrees of hydrologic connectivity (Smith and Pavelsky 2009). A water mask for PAD was derived from an 17 August 1999 Landsat scene with 28.5 m spatial resolution (T. Pavelsky, personal communication) (see figure 1(*a*)). It consists of 1274 water bodies with surface areas ranging from 0.01 km^2 to 1249 km^2. Two other study areas represent the Arctic region where substantial changes in the terrestrial water cycle have been observed over the last century due to climate change (Peterson *et al.* 2002, Smith *et al.* 2005). The water mask over the Arctic Coastal Plain (ACP) of Northern Alaska was extracted from 1 July 2001 Landsat imagery with 28.5 m spatial resolution (see figure 1(*b*)). It consists of 20 501 lakes with surface areas ranging from 0.01 km^2 to 587 km^2. The water mask over West Siberia is generated using the Russian RESURS-1 satellite image with 150 m spatial resolution acquired during summer of 1997 (see figure 1(*c*)). It consists of 35 090 lakes with surface areas ranging from 0.06 km^2 to 171 km^2.

2.2 *Simulation of SWOT water surface height data*

2.2.1 Satellite radar altimetry processing. Satellite radar altimetry has been used for water elevation monitoring over large inland water bodies such as the Great Lakes (Morris and Gill 1994, Birkett 1995) and the Amazon basin (Birkett 1998, Birkett *et al.* 2002). These large lakes have scattering characteristics similar to the ocean surface, such that range measurements from the nominal tracking mode in the Geophysical Data Record (GDR) yield accurate height measurements, albeit at single points. Recently, retracked TOPEX/POSEIDON and Envisat altimetry measurements have been used to monitor water level variations in Louisiana's vegetated wetlands (Kim *et al.* 2009, Lee *et al.* 2009).

In this study, we use retracked Envisat 18-Hz data (~350 m along-track sampling) to measure water elevation changes over lakes defined by the water masks. The Envisat altimeter data used in this study are from the periods of September 2002 to September 2008. Envisat orbits on a 35-day repeat cycle with $98.5°$ inclination, and achieves coverage from $81.5°$S to $81.5°$N. We carefully select each 18-Hz measurement because most of the lakes are relatively small in size compared to the radar footprint, which can be several kilometres in diameter depending on the surface roughness. Lake size distributions for each study region are shown in figure 2. As
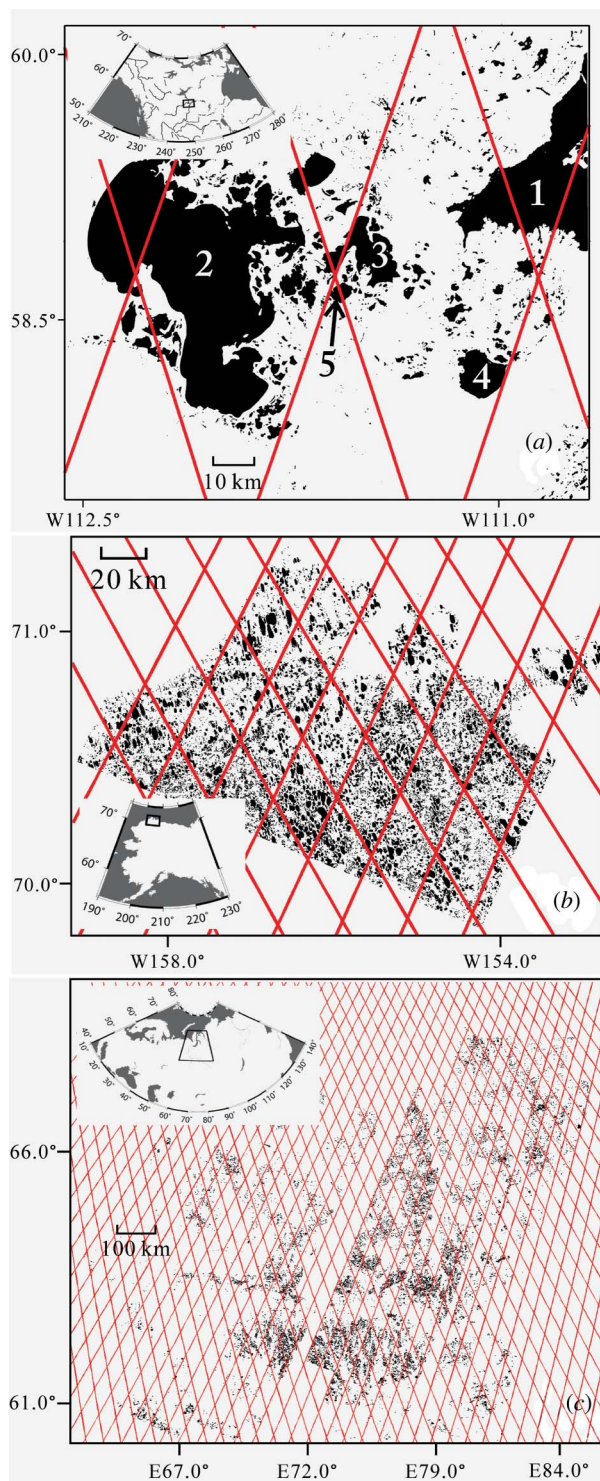
Figure 1.   Water mask with Envisat tracks over (*a*) PAD (1: Lake Athabasca, 2: Lake Claire, 3: Lake Mamawi, 4: Lake Richardson, 5: Otter Lake), (*b*) Alaska, (*c*) Siberia.
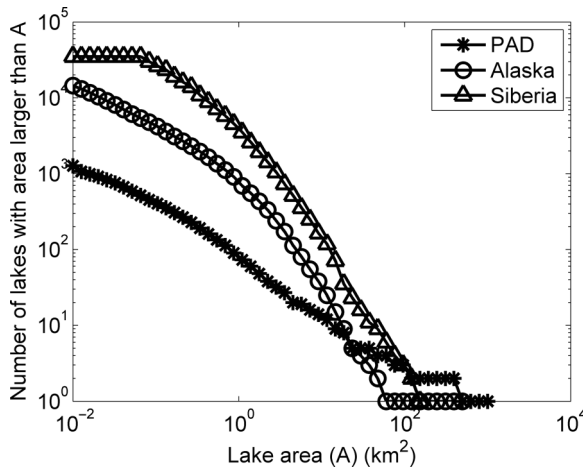
Figure 2.   Lake size distribution based on the water mask of the study areas.

observed in other studies (Lehner and Döll 2004, Downing *et al.* 2006), the distributions follow a power law in the form of $N = xA^y$.

To locate lakes for which we have reliable Envisat measurements, we selected lakes larger than the nominal footprint of the Envisat altimeter (~2.5 km in diameter). Then, along each Envisat 18-Hz ground track location, we intersect a circle with an area equivalent to the footprint size with the lake mask to determine the fraction of each Envisat measurement that is over water (figure 3). Water elevation at a given time is obtained from an average of Envisat measurements for a given pass that fall within the lake, weighted by fraction of the Envisat footprint within the lake polygon as:

$$h_{t,\text{observed lake}} = \frac{\sum_{i=1}^{n}(w_i h_i)}{\sum_{i=1}^{n} w_i} \text{ with}$$

$$w_i = \frac{\text{Area of Envisat footprint intersected with a lake}}{\text{Area of Envisat footprint}},$$

(1)

where $h_{t,\text{observed lake}}$ is the weighted average of Envisat 18-Hz water elevation observations, h_i, over a lake. Figure 3 shows examples of the time series of water elevation anomaly over the study regions observed from Envisat. It should be noted, however, that the presence of snow and ice on the lake surface, which may persist for a significant fraction of the year, perturbs the altimeter measurements by volume scattering of the media and two-way attenuation of the radar signal (Papa *et al.* 2002, Kouraev *et al.* 2004). Therefore, the altimeter measurements during the winter may become less reliable and should be interpreted with caution.

2.2.2   Creating surface water elevation for unobserved lakes.   Conventional profiling repeat-track radar altimeters have wide orbital spacing; for example, 35-day repeat Envisat tracks are approximately 40, 25, and 30 km apart between two successive ascending or descending tracks over PAD, Alaska, and Siberia, respectively. For TOPEX/Poseidon, which has a 10-day repeat period, the gaps are greater than
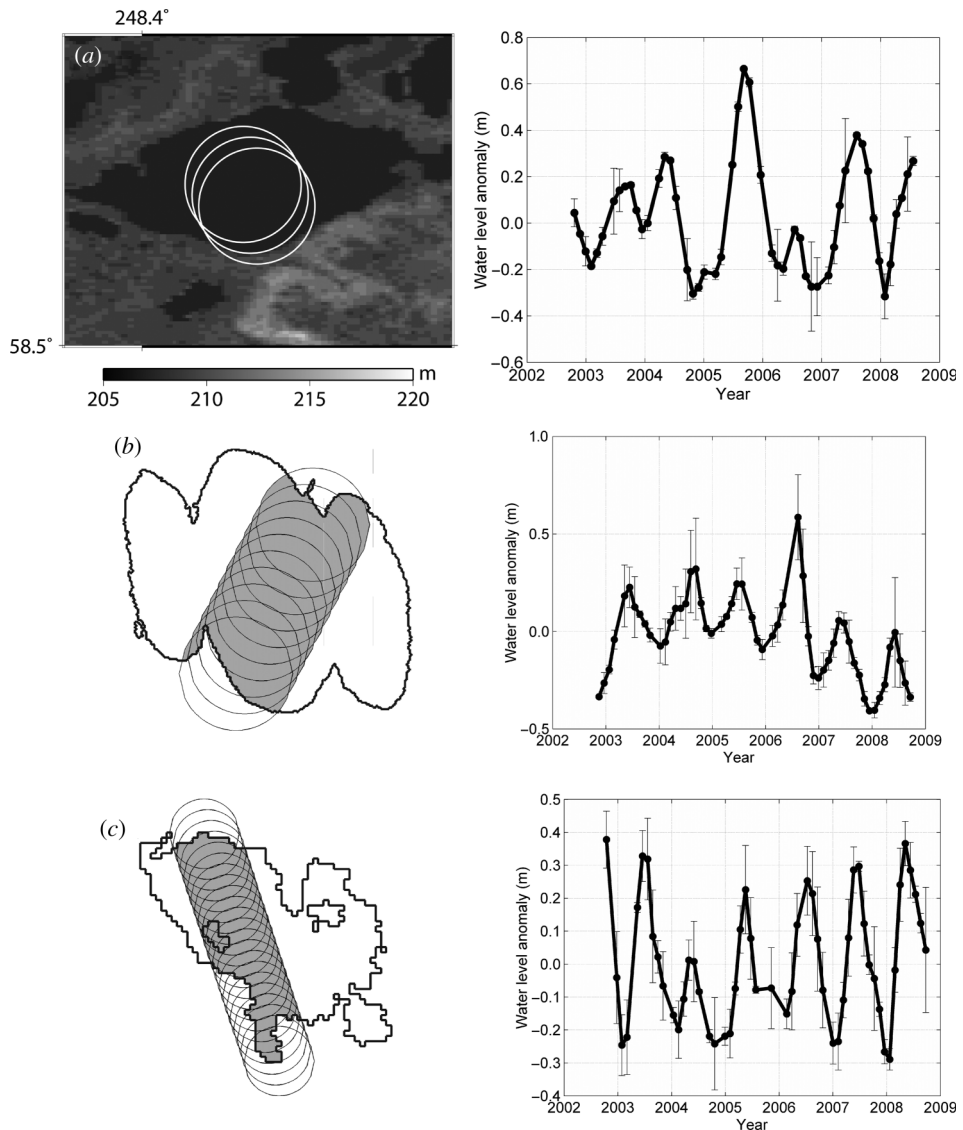
Figure 3. Examples of Envisat-observed water elevation anomaly over (*a*) PAD, (*b*) Alaska, (*c*) Siberia.

those of Envisat by approximately a factor of three. Therefore, conventional altimeters miss most of the water bodies in the study areas, whereas SWOT will observe all of the water bodies. In order to simulate SWOT coverage, we synthesize an estimate of the water elevation changes for the unobserved lakes. Smith *et al.* (2005) showed spatially heterogeneous patterns of disappearing lakes. Over a ~30 year period, lakes separated by only a few kilometres have significantly different rates of storage changes. Hence, we create water elevation changes reflecting this heterogeneous spatial distribution using the water elevation changes over Envisat-observed lakes. By examining the time series of individual observed lakes, the annual flood due

to spring melt can be clearly observed (figure 3), thus a sinusoid with annual frequency can be fitted to characterize and quantify this underlying hydrologic process. For each Envisat-observed lake, the time series of water elevation anomaly can be expressed as:

$$h_{t,\text{observed lake}} = \bar{\bar{h}}_t + h'_{t,\text{observed lake}}, \qquad (2)$$

where $h_{t,\text{observed lake}}$ is the water elevation anomaly at time t, $\bar{\bar{h}}_t$ is the sinusoid with annual frequency ($= H \sin \omega t$, $\omega = 2\pi/1\text{year}$) fitted using all water elevation anomaly time series, and $h'_{t,\text{observed lake}}$ is the residual at time t. Figure 4(a) shows the Envisat-observed water elevation anomaly time series with the fitted sinusoid for Envisat-observed lakes in PAD. The time series shows high water during 2005 and low water during 2006. This agrees with the fact that water levels on the Peace and Athabasca Rivers were notably higher during 2005 but significantly lower during 2006, resulting in substantial lake recharge in 2005 and little recharge in 2006 (Pavelsky and Smith 2008). The residuals, $h'_{t,\text{observed lake}}$ (figure 4(b)), represent the spatiotemporal variability inherent in the observed lakes, which includes not only the interannual variability, but also the spatial variability among the lakes. At each time t, a value, $\hat{h}'_t$, is randomly selected between the minimum and maximum values of the residuals (figure 4(c)), and added back to the fitted sinusoid $\bar{\bar{h}}_t$, to simulate the water elevation
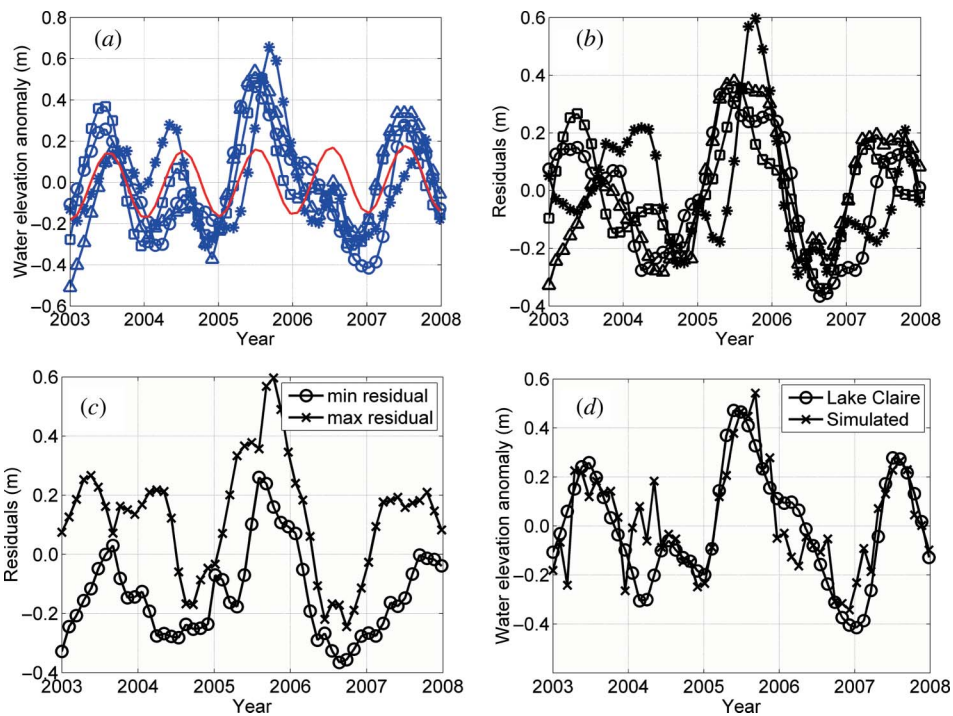
Figure 4. Creating water elevation anomalies for the unobserved lakes; (a) Envisat-observed 35-day interval time series over Otter Lake (star), Lake Claire (circle), Lake Richardson (square), and Lake Mamawi (triangle). Red line shows the fitted sinusoid with annual frequency; (b) time series of the residuals for each Envisat-observed lake; (c) minimum and maximum of the residuals at epochs with 35-day interval; (d) example of a created time series as described in §2.2.2. Time series of the Lake Claire is shown for comparison.

anomaly time series for every unobserved lake (figure 4(*d*)). As noted above, the lakes in some of these environments, notably PAD, are characterized by varying degrees of hydrologic connectivity (Smith and Pavelsky 2009), which lead to different water level variations from lake to lake. Our method does not take hydrologic connectivity into account; thus, the water elevations constructed by this technique should be interpreted with caution for purposes other than characterizing SWOT storage change measurement errors, which is the main goal of this study. However, the water elevations estimated for lakes without altimeter observations have two key characteristics: (1) they follow the annual cycle including rising water during spring due to snowmelt events; and (2) they lie within the observed range of water elevation fluctuations.

2.2.3 Creating daily water elevation changes.   The time series of water elevation anomalies described above was generated with the same 35-day temporal resolution as Envisat, while SWOT will measure lakes more frequently. Hence, we need to create daily estimates of truth to avoid aliasing in the subsequent SWOT sampling. To do so, we extract high-frequency components (i.e. with a period less than 35 days) from *in situ* daily gauge measurements and add them to the original time series. There is only one gauge with long-term daily measurements in our study regions; it is located in Lake Athabasca in PAD. Therefore, we assume that lakes in other study regions will have similar high-frequency level variations due to similar controlling hydrologic processes, e.g. the diurnal behaviour of snowmelt-forced discharge in some regions (Hardy 1996). However, it should be noted that our assumption of Lake Athabasca's representativeness might be incorrect because daily variations in water level on Lake Athabasca during the open water season are strongly influenced by wind, unlike smaller lakes in the study region (T. Pavelsky, personal communication). It is also possible that the high water events which may last for less than 35 days cannot be reconstructed using the Envisat measurements. Figure 5(*a*) shows water elevation anomalies from 35-day Envisat observations and daily gauge measurements in Lake Athabasca near Crackingstone Point. The correlation coefficient and root mean square error (RMSE) between them are 0.95 and 11.84 cm, respectively. This high level of agreement helps to validate the Envisat measurements. Figure 5(*b*) shows their power spectra and indicates that the daily gauge measurements contain higher frequency components. Figure 5(*c*) shows the time series after adding the high frequency components extracted from the daily gauge measurements along with the original time series from the 35-day interval observations. A subset of the time series is shown in figure 5(*d*), for clarity. The daily water elevation changes over all of the water bodies in the study regions for a period of 5 years were generated following this method. Figure 6 shows an example of the created true water elevation anomaly map at Day 120 (or 30 April 2002) over the study regions.

2.3 *SWOT orbit overlay: spatiotemporal sampling*

Once the true water elevation anomaly maps are generated, SWOT orbital tracks with different spatial and temporal sampling are overlain on the maps in order to simulate SWOT observations. Note that SWOT is a wide-swath altimeter with a swath width of 140 km. Currently, SWOT is planned to have two operational phases: the 'fast phase' will have a 3-day repeat period and will take place during the first three to six months of mission operations, whereas the 'nominal phase' will have a 22-day exact repeat period which is planned for three years of mission operations. The fast phase will have more frequent revisit times, but the spatial coverage will be limited, while the nominal
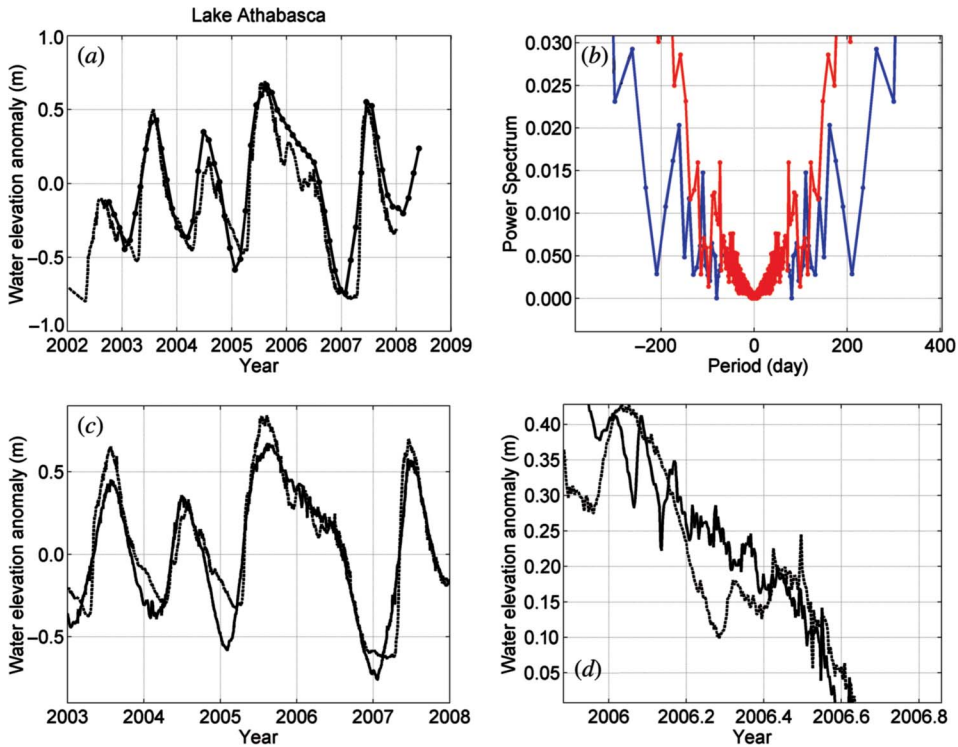
Figure 5. Creating daily water elevation changes; (*a*) comparison of water elevation anomalies between *in situ* daily gauge (dashed) and Envisat measurement with 35-day interval (solid) over Lake Athabasca; (*b*) power spectrum of *in situ* daily gauge (red) and Envisat measurement with 35-day interval (blue) over Lake Athabasca. Note that Envisat time series does not have the high frequency components corresponding to less than 70-day period; (*c*) comparison of water elevation anomalies between *in situ* daily gauge (dashed) and Envisat measurement with high-frequency components (solid); (*d*) zoomed time series for clarity.

phase will have less frequent visits, but global coverage. Because of swath mapping, revisits will occur at least twice during a repeat period at any given location during the nominal phase (Alsdorf *et al.* 2007). Along with the 22-day repeat period orbit for the nominal phase, 15- and 21-day repeat orbits were also considered as candidate SWOT orbits. The candidate orbits were chosen to avoid ocean tidal aliasing or aliasing of the seasonal signals, which occurs when a tidal signal is sampled with a longer period (Parke *et al.* 1987) or the aliased tidal period is the same as the seasonal period. The orbital inclinations considered in this study are 74° and 78°. The inclination angle (*i*) determines the turning latitude (ϕ_{max}) of the satellite ($|\varphi_{max}| = i$, for a prograde orbit), and therefore the latitudinal range over which the Earth surface is to be measured. Because of the convergence of the orbits, 74° inclination provides more frequent revisit times over the Arctic basins, whereas the orbit with 78° inclination can capture the entire Arctic Ocean at the higher latitudes (see figure 2 in Biancamaria *et al.* 2010). Consequently, the SWOT spatiotemporal sampling is sensitive to the choice of orbital inclination. In this study, we consider eight orbits based on different permutations of four exact repeat periods (3-, 15-, 21- and 22-day) and two orbital inclinations of 74°
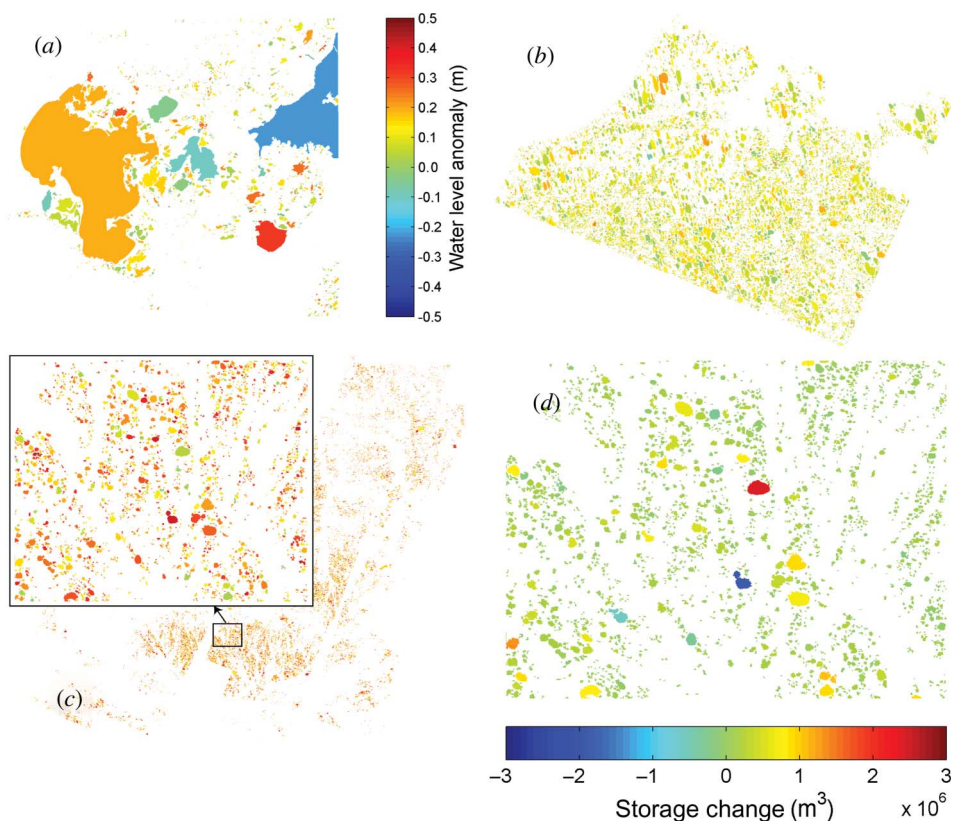
Figure 6. Created 'true' water elevation anomaly at Day 120 (or 30 April 2002) over (*a*) PAD, (*b*) Alaska, (*c*) Siberia, (*d*) true storage change of Siberian lakes in the rectangle shown in (*c*).

and 78°. Figure 7 shows the swath coverage for an entire SWOT cycle constructed using the 22-day exact repeat period and a 78° inclination orbit.

Once the days on which the measurement occurs are determined for every water body, the height measurement error of the SWOT instrument is added to the true water elevation changes generated in the previous section. In this study, we make the conservative assumption that the SWOT interferometric synthetic aperture radar samplings (e.g. pixels) are 50 m by 50 m with a zero mean Gaussian random height errors having a standard deviation σ_h of 0.5 metres. In reality, SWOT pixels will have smaller sizes ranging from 10 m to 60 m in the cross-track direction and as small as 2 m in the along-track direction. As described by Durand *et al.* (2008), random and systematic measurement errors of SWOT derive from several sources, including thermal noise, errors due to imperfect modelling of dry and wet troposphere and ionosphere delays, systematic height errors due to spacecraft roll, and layover due to topography and vegetation. In this study, we focus on the first-order errors which are the errors due to spatiotemporal sampling, random height errors resulting from thermal noise, and inundated area measurement errors. Future studies will investigate the other error sources. Because random height measurement errors are additive, averaging of the height measurements of every pixel over the water body reduces the error standard deviation (Moller *et al.* 2008):
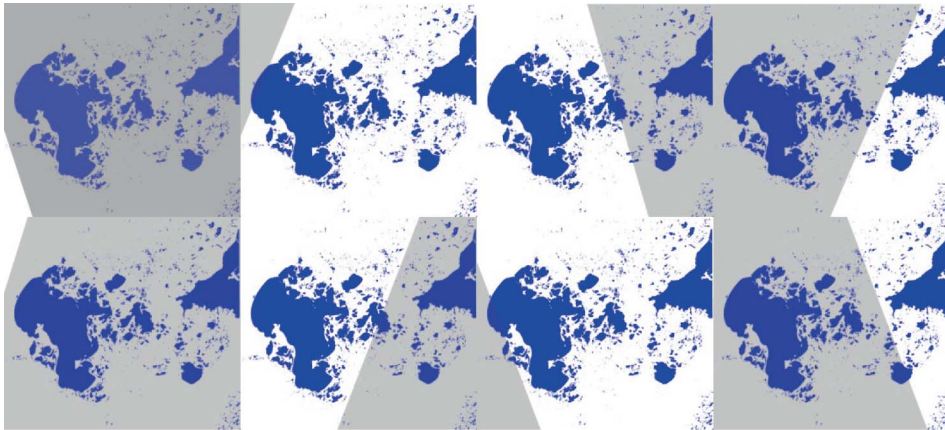
(*a*)
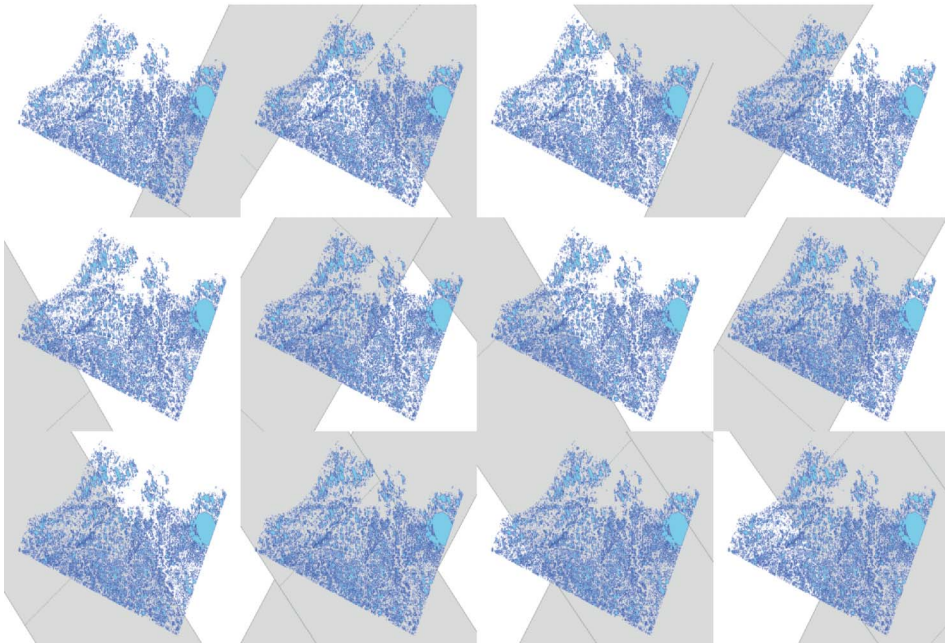
(*b*)

Figure 7.   SWOT measurement swaths from the 22-day repeat period and 78° inclination orbit over (*a*) PAD for days 2, 4, 5, 7, 10, 13, 18, and 21 (from left to right and top to bottom); (*b*) Alaska for days 2, 3, 5, 6, 7, 9, 10, 12, 13, 15, 18, and 21 (from left to right and top to bottom); (*c*) Siberia for days 1, 2, 3, 4, 5, 7, 8, 9, 10, 11, 12, 13, 14, 15, 16, 17, 18, 19, 20, 21, and 22 (from left to right and top to bottom).

$$h_{err} \sim N\left(0, \frac{1}{\sqrt{n_{obs}}} \sigma_h\right), \tag{3}$$

where n_{obs} is the number of SWOT pixels over a lake and can be computed by dividing the lake area obtained from the mask by the area of the SWOT pixel (50 m by 50 m). It is therefore apparent that a relatively larger lake can be more accurately measured
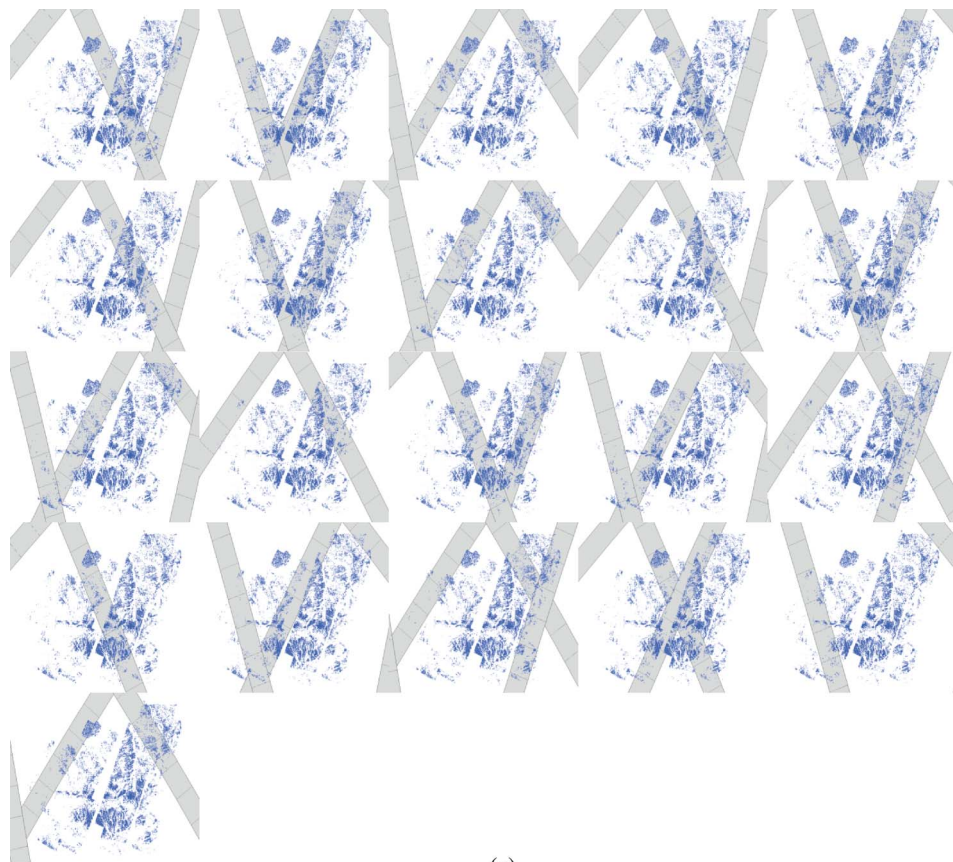
(*c*)

Figure 7.   (*Continued.*)

than a smaller lake. For example, figure 8(*a*) shows the distribution of RMSE between
true and SWOT-observed water elevation anomalies over all of the lakes in PAD
using a 22-day repeat period and 78° inclination orbit. SWOT accuracy is approxi-
mately 2 cm RMSE over lakes larger than 1 km^2. SWOT accuracy for lakes of size 250
m × 250 m is approximately 8 cm RMSE over PAD. Figure 8(*b*) is an example of a
simulated true and SWOT-observed water elevation anomaly time series over a lake in
PAD for a 22-day repeat period and 78° inclination orbit.

2.4   *SWOT-observed inundated area*

The error in the inundated area measurements from SWOT will be mainly due to the
edge effects around the lake shores, and can be modelled using the size and shape of
the water body and the imaging resolution of SWOT. A water body image taken by
the sensor consists of discrete pixels, and the imaging process thus causes both
commission and omission errors at the boundary cells. These commission and omis-
sion errors are always the smaller portion of the bisected cells by the shore. If the
bisected cell is included as water, then a commission error occurs. Otherwise, the
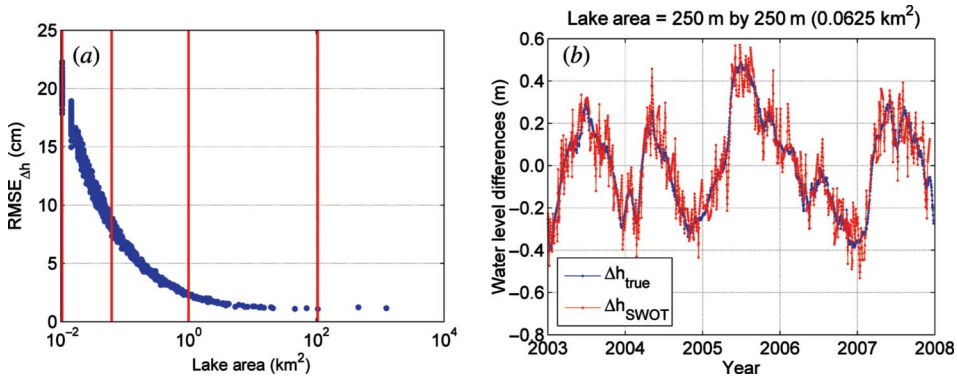
Figure 8. (*a*) RMS error of the SWOT-observed water elevation change over all of the lakes in PAD. Red vertical lines indicate the lakes of sizes 100 m × 100 m, 250 m × 250 m, 1 km × 1 km, and 10 km × 10 km. (*b*) Example of simulated 'true' and SWOT-observed water elevation change time series over a lake of size 250 m × 250 m in PAD. 22-day repeat period and 78° inclination angle orbit is used.

water portion is ignored, and an omission error occurs. Hence, the areal error of a water body can be estimated from the summation of the commission and omission errors for all of the boundary cells around the water body. This is the classical 'mixed-pixel' problem. The error for one cell is equal to the root mean square of the smaller area obtained when a random straight line is laid across the cell (Crapper 1980). Assuming the line segment in the cell is a straight line, the areal error can be approximated as (for details see Sheng (2008)):

$$\sigma_A = 0.2359 \frac{R^{\frac{3}{2}} A^{\frac{1}{4}}}{(\text{CI})^{\frac{1}{2}}}, \tag{4}$$

where CI is the compactness index of the water body, R is the pixel size of SWOT, and A is the true inundated area. CI and A can be computed using the water masks, and R is assumed to be 50 m. SWOT-observed inundated area can be characterized by adding zero mean Gaussian random errors with a standard deviation of σ_A to the true inundated area. We did not consider the lateral variations of the inundated area in time, i.e. the variations of the shoreline with water elevation change; this indicates a need for future studies to generate more realistic inundated area. However, the goal of this study is not to completely recreate reality, which would require the actual SWOT satellite, but rather to make statistically reasonable estimates of storage changes and to use these to study the feasibility of the SWOT satellite repeat period and orbital inclination.

2.5 SWOT-observed storage changes

SWOT-observed storage changes are computed by multiplying the SWOT-observed water elevation changes with the SWOT-observed inundated area. Although the number of SWOT revisits can reach more than 10 times during the repeat period over our study regions (see figure 9), SWOT will not provide daily storage change estimates during the nominal phase of the mission (note that SWOT sampling may be daily for some locations during the fast-sampling phase of the mission). Since for
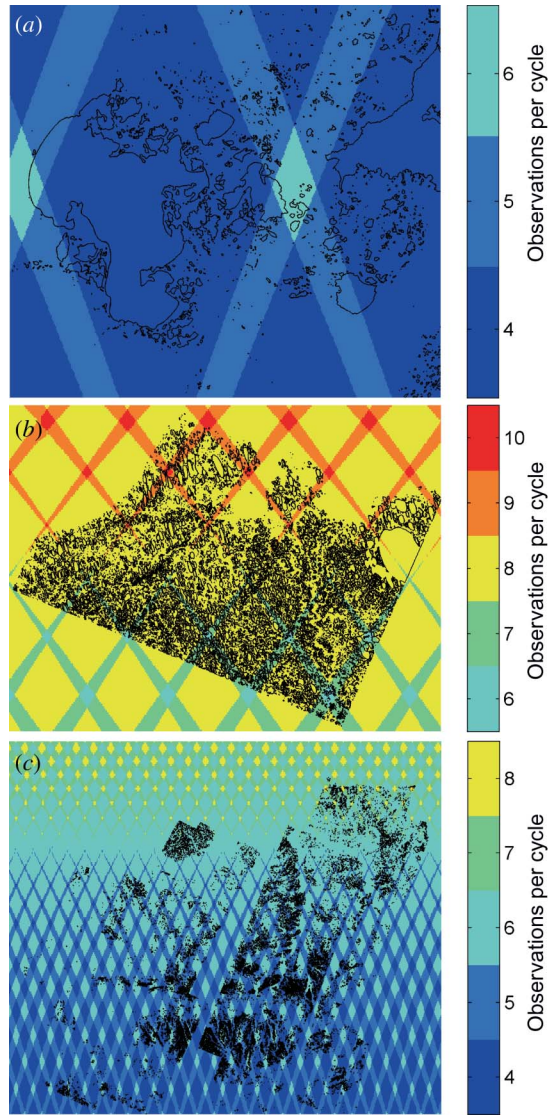
Figure 9. Number of observations per cycle over (*a*) PAD, (*b*) Alaska, and (*c*) Siberia using 22-day repeat period and 78° inclination orbit.

Arctic regions many lakes show strong seasonal cycles (e.g. figure 3), monthly storage changes are examined in this study using the monthly averaged water elevation changes:

$$\Delta S_i^{j\text{th month}} = A_i \Delta h_i^{j\text{th month}} = A_i \left(h_i^{j\text{th month}} - h_i^{(j-1)\text{th month}} \right) \quad (5)$$

where $\Delta S_i^{j\text{th month}}$ is the monthly storage change estimate over lake i at the jth month, A_i is the inundated area of lake i, $\Delta h_i^{j\text{th month}}$ is the monthly water elevation change over lake i at jth month, and $h_i^{j\text{th month}}$ is the monthly averaged water level anomaly over lake i at the jth month.

3. Results and discussion

3.1 *Storage change errors of SWOT*

The differences between the true and SWOT-estimated storage changes will yield a time series of absolute storage change error over a specific lake. Subsequently, a time series of relative storage change error for the lake can be obtained as:

$$\varepsilon^{\text{relative}}_{\Delta S_i^{j\text{th month}}} = \frac{\varepsilon^{\text{absolute}}_{\Delta S_i^{j\text{th month}}}}{\text{Range}(\Delta S_i)}, \tag{6}$$

where $\varepsilon^{\text{relative}}_{\Delta S_i^{j\text{th month}}}$ and $\varepsilon^{\text{absolute}}_{\Delta S_i^{j\text{th month}}}$ are the relative and absolute storage change errors over the lake i at the jth month, respectively, and $\text{Range}(\Delta S_i)$ is the range of true storage changes over lake i over the entire study period.

Figure 10 illustrates examples of monthly true and SWOT-estimated storage change time series over the study regions using the 22-day repeat 78° inclination orbit. Because of the resolution of the RESURS-1 satellite image used to derive the water mask, the minimum lake size in Siberia is 150 m × 150 m, which is larger than PAD or Alaska study areas. The SWOT-estimated storage changes agree with the true storage changes for large lakes. SWOT also demonstrates a promising capability to measure the storage changes for very small lakes, such as those that are less than 250 m × 250 m. To have a representative number of absolute and relative storage change errors for each lake, the standard deviations of their time series are computed. Figure 11 shows the distribution
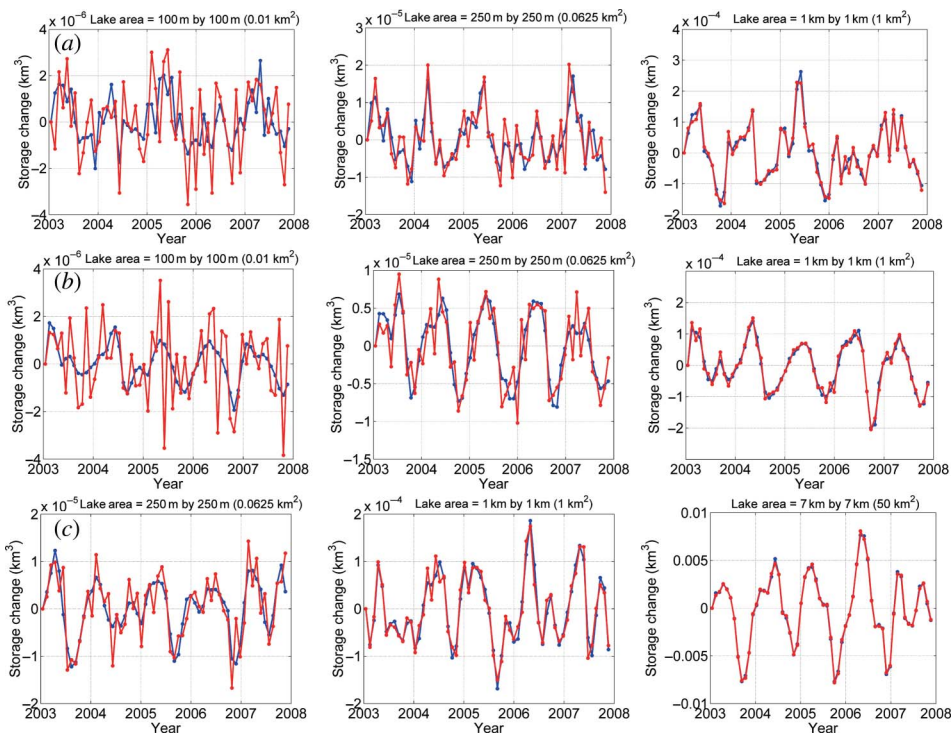
Figure 10. Examples of monthly true (blue) and SWOT-estimated (red) storage changes over (*a*) PAD, (*b*) Alaska, and (*c*) Siberia.
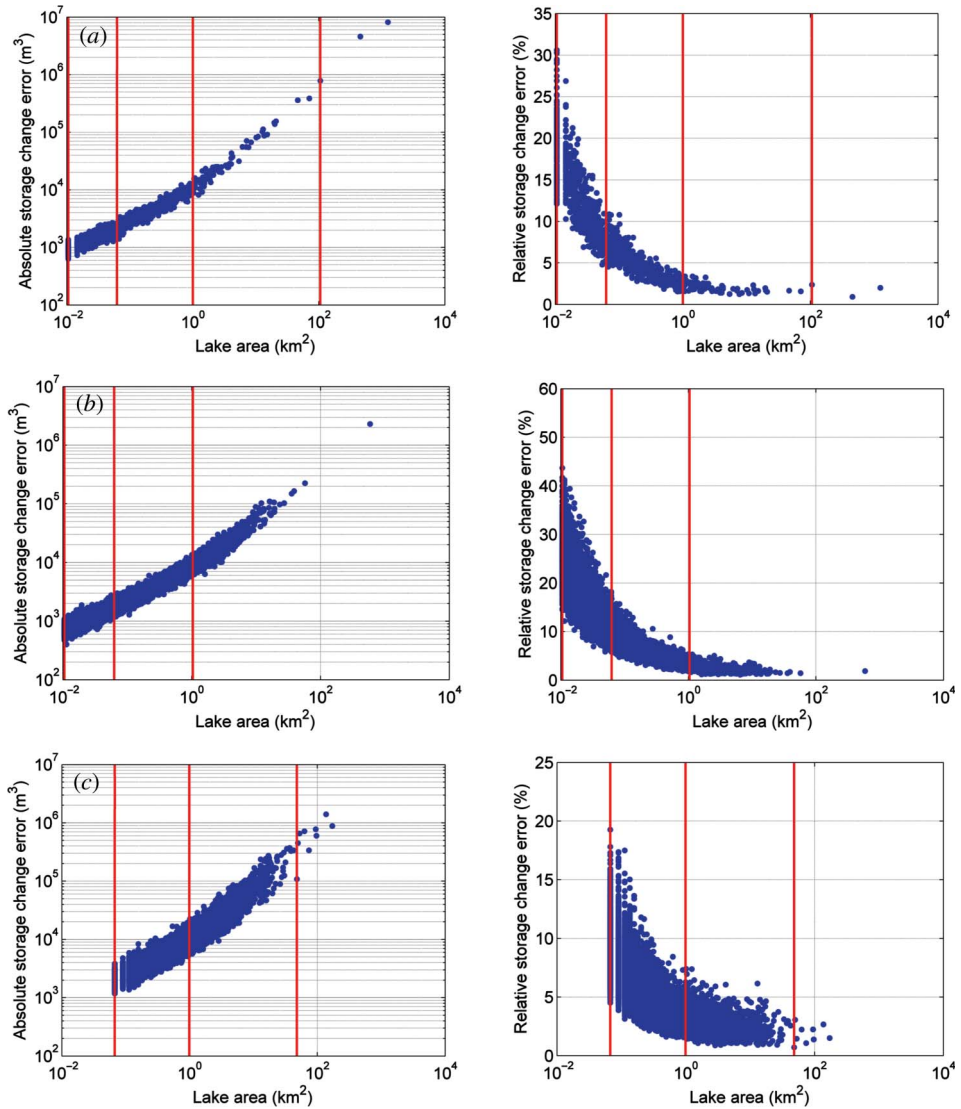
Figure 11.   Absolute and relative storage change errors of SWOT using 22-day repeat period and 78° inclination orbit over (*a*) PAD, (*b*) Alaska, and (*c*) Siberia. The red lines indicate the areas of the lakes which are used for examples in figure 10.

of the absolute and relative storage change errors with respect to the lake sizes using the same orbit. While the absolute storage change error becomes larger as the lake size increases, the relative storage change error becomes smaller. The relative storage change errors for 1 km^2 lakes are generally less than 5% for all three study regions, while errors for smaller lakes of 100 m $\times$ 100 m are generally about 20% (range is from a minimum of 5% in Siberia to a maximum of 40% in Alaska).

  Table 1 summarizes the median of the relative storage change errors over the study regions using eight different SWOT orbits. The fast phase orbits with 3-day repeat period provide marginally improved accuracies over the nominal phase orbits, but the

Table 1. Estimated storage change errors over the study regions using different SWOT orbits (these are the median percentage errors encompassing all lake sizes, see §3.1). The percentages in the parenthesis indicate the portion of the lakes missed by the fast phase orbit. They are representative numbers as they can vary with different nodal crossings chosen to generate the fast phase orbital tracks. Different nodal crossings create different fast phase orbital coverages, which result in different spatiotemporal samplings. Therefore, they are representative for comparisons amongst the two inclination angles.

	Storage change error (%)		
	PAD	Alaska	Siberia
22-day 78° orbit	8.9	12.8	5.4
21-day 78° orbit	9.1	14.4	5.3
15-day 78°orbit	9.1	12.1	5.1
3-day 78° orbit	7.1 (15% missed)	9.0 (22% missed)	4.5 (33% missed)
22-day 74° orbit	8.5	10.1	5.1
21-day 74° orbit	8.4	9.9	5.0
15-day 74° orbit	8.3	9.7	4.9
3-day 74° orbit	7.2 (3% missed)	9.4 (17% missed)	4.3 (30% missed)

fast phase orbits result in limited spatial coverage, as described in §2.3. Note that Siberia shows relatively smaller storage change errors than PAD or Alaska because of the different smallest lake sizes. All potential SWOT orbits result in similar storage change errors of ~5% over Siberia. Comparing the 74° and 78° inclinations and 15-, 21- and 22-day exact repeat periods, the monthly storage change errors over Siberia are not significantly sensitive to the repeat periods or inclinations of the orbit. Similarly, the storage change errors over PAD are rather insensitive to the orbital configurations. Storage change errors over Alaska vary slightly with different orbit inclination angles and repeat periods. The differences in the storage change errors obtained from various orbital inclinations and repeat periods are relatively small, thus this study demonstrates that there is no preferential choice amongst the potential SWOT orbits.

3.2 *Contribution of SWOT areal error*

The remainder of this investigation is focused on understanding the variability of the storage change errors shown in table 1. We investigate the contribution of the SWOT areal error in this section and SWOT water elevation measurement error in the next section. Combined, these are the two contributors to the storage change error.

From table 1, it is counterintuitive that the storage change errors are relatively larger in Alaska than in PAD because Alaska is located at higher latitude and the lakes in Alaska thus have more frequent revisit times (see figure 9). To proceed, we examine the error in SWOT-observed inundated area. From equation (4), the areal error decreases as the lake size increases. In figure 12(*a*), areal errors in Alaska are larger than those of PAD when comparing lakes of the same size. The only factor that can cause the difference in the areal error is the compactness index, CI in equation (4). The compactness index is defined as the ratio of the area of a polygon to the area of a circle with equal circumferences; CI can be computed as $2\sqrt{\pi A}/L$, where A and L are the area and perimeter of the polygon, respectively. The compactness index is used to numerically describe the shape of the polygon, and theoretically, for a circle, it is
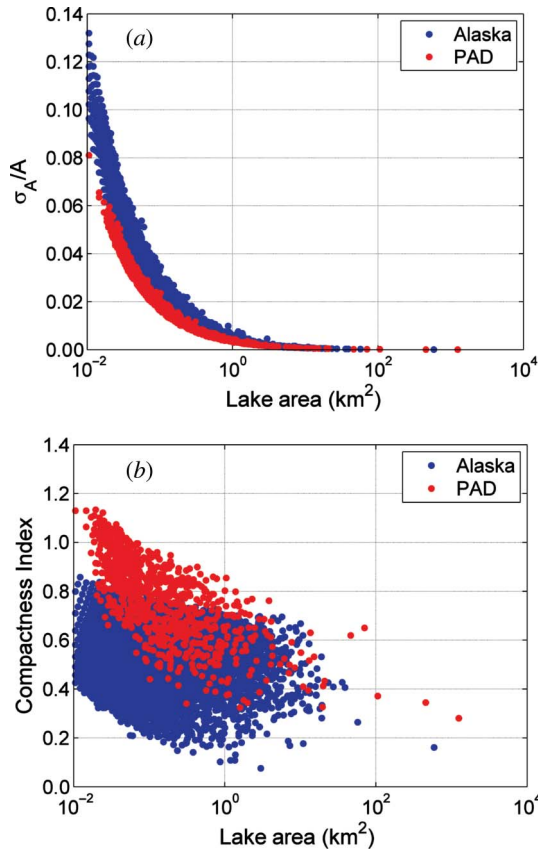
Figure 12. Comparison of (*a*) areal error and (*b*) compactness index between PAD and Alaska.

equivalent to 1. Figure 12(*b*) shows that the lakes in PAD have relatively higher compactness indexes than Alaska. This implies that Alaska has a greater number of elongated lakes than PAD, which results in smaller areal error for PAD lakes, according to equation (4). This result indicates that the shape of the water body is an important contributing factor in estimating the storage change error.

3.3 *Contribution of SWOT temporal sampling*

Orbits with a 74° inclination yield smaller storage change errors than orbits with a 78° inclination over Alaska (table 1). Furthermore, relatively larger storage change error is obtained from the orbit with 21-day repeat period and 78° inclination than from the orbit with 15- or 22-day repeat period and 78° inclination. While these differences are small, it is important to investigate their sources. We explore the differences in the storage change errors over Alaska in terms of the differences in SWOT temporal sampling, which in turn is due to the orbital inclination and repeat period.

3.3.1 Orbit inclination angle. The main difference between the 74° and 78° inclination orbits is the coverage at high latitudes (Biancamaria *et al.* 2010). This is due to the convergence of the orbit near the turning latitude and the swath sampling of

SWOT. Thus, the orbital inclination plays an important role in the number of revisits over our study area in Alaska located near 71° N. The 74° inclination orbit (figure 13(*b*), left) provides more observations for the 22-day repeat period than the 78° inclination orbit (figure 13(*a*), left). Furthermore, the medians of the temporal sampling gaps are also computed for each lake because the SWOT sampling is not uniformly distributed in time during one repeat period (Biancamaria *et al.* 2010). From figure 13, 18.9% of the lakes in Alaska have a median temporal sampling gap of 1 day for the 74° inclination orbit, whereas all of the lakes have a median temporal sampling gap larger than 2 days for the 78° inclination orbit. It is expected that larger
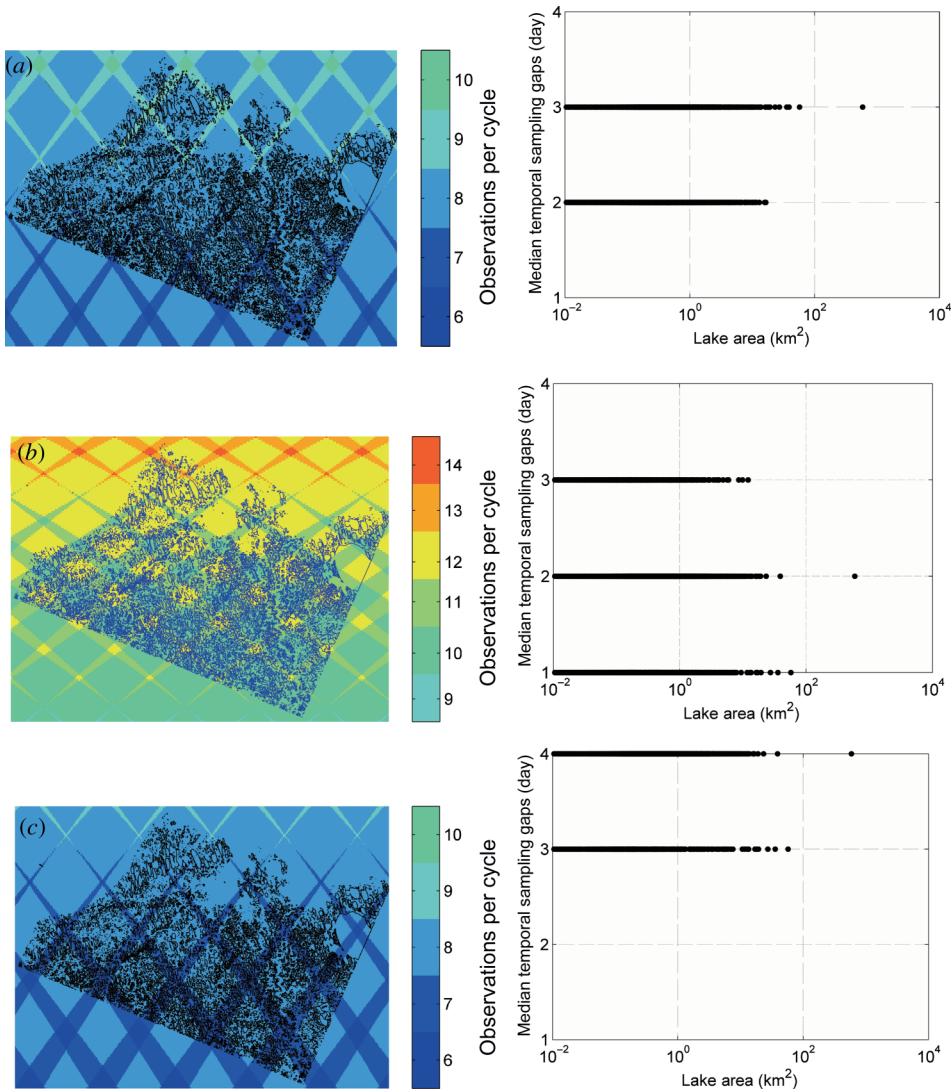

Figure 13. Orbit analysis over Alaska with different orbit inclinations and repeat periods: (*a*) 22-day repeat period and 78° inclination orbit, (*b*) 22-day repeat period and 74° inclination orbit, (*c*) 21-day repeat period and 78° inclination orbit. Left panels show numbers of observations per cycle.

temporal sampling gaps will lead to larger RMSE of SWOT-observed water elevation change, and consequently larger storage change error estimates. In summary, the orbital inclination drives the difference in the storage change errors over Alaska because it is located near the turning latitude of the 74° inclination orbit and accordingly yields different temporal samplings.

3.3.2 Orbit repeat period. The exact repeat period of the orbits (figures 13(*a*) and 13(*c*)) can also lead to the differences in the temporal sampling gap, although there are no apparent differences in the number of observations per repeat period. This confirms the need to examine not only the number of revisits, but also the temporal sampling gap. Using 22-day repeat 78° inclination orbit, 31% and 69% of the lakes in Alaska have median temporal sampling gaps of 2 days and 3 days, respectively. If the 21-day repeat 78° inclination orbit is used, 10% and 90% of the lakes in Alaska have median temporal sampling gaps of 3 days and 4 days, respectively. As a result, the 21-day repeat period and 78° inclination orbit results in larger storage change error estimates over Alaska than 22-day repeat period and 78° inclination orbit.

To summarize, the RMSE of the SWOT-observed water elevation change depends on the temporal sampling of the SWOT orbit: how frequently it is sampled, and how large the temporal gap is between the sampling. Figure 14 illustrates how the RMSE changes with different inclination angles and repeat periods over Alaska. As can be
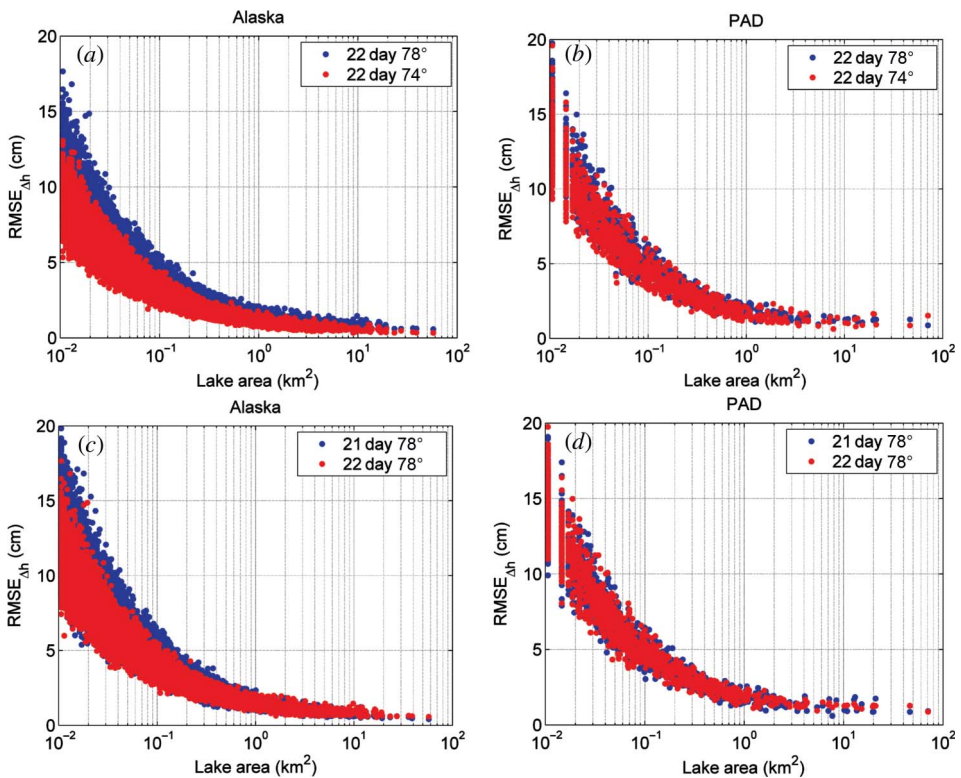

Figure 14. RMSE of SWOT water elevation changes over Alaska and PAD using (*a*) 22-day repeat period and 74°/78° inclination orbits, (*b*) 21-/22-day repeat period and 78° inclination orbits.

seen from figure 14(*a*), overall, lower RMSE is obtained over the lakes in Alaska (left) using 74° inclination orbit than using 78° inclination orbit. Similarly, figure 14(*b*) shows that the orbit with 22-day repeat 78° inclination angle generates lower RMSE over Alaska (left) than the orbit with 21-day repeat 78° inclination angle. Conversely, none of the orbital configurations result in significantly different RMSE over PAD. In conclusion, the difference in temporal sampling and thus the RMSE of the SWOT-observed water elevation change explains the sensitivity of the storage change estimates to different SWOT orbit configurations.

4.   Summary and conclusions

In this study, we have characterized the expected error of monthly storage change estimates from SWOT measurements in three study regions: PAD, Northern Alaska and Western Siberia. We have modelled errors due to random height measurements, random areal measurements due to edge effects, and error due to the SWOT spatio-temporal sampling. A conservative assumption on the wide-swath instrument pixel size of 50 m × 50 m and height measurement error of 50 cm has been made. True daily water elevation change maps are simulated for a period of 5 years using Envisat radar altimetry and daily *in situ* gauge measurements. Various SWOT orbits with different repeat periods and inclination angles are overlain over the generated water elevation map. The number of revisits increases with latitude from four to eight per 22-day cycle over the study areas. The SWOT-observed water elevation change from this spatio-temporal sampling is combined with the SWOT-observed inundated area estimated using the areal error model to yield SWOT-estimated storage changes.

We analysed the differences in the storage change estimates due to different orbit configurations between study regions and within study regions. SWOT storage change accuracy is primarily controlled by lake size such that the monthly error is generally less than 5% for lakes larger than 1 km^2 and is about 20% for lakes of around 1 ha. The areal error due to lake shape can play a role in the storage change error differences between study regions. Temporal sampling and consequently the SWOT-observed elevation change error is the factor contributing to the differences in the storage change estimates within a study region. In particular, PAD and Siberia have similar storage change estimates regardless of the different orbit sampling. In general, our results demonstrate that SWOT water level and storage change measurements are relatively insensitive to both the orbital inclination and the orbital exact repeat period. However, this sensitivity is generally latitude-dependent, with the northernmost areas being only slightly sensitive to the choice of orbit. Even for areas such as the Alaska study region, however, there is very little difference between the 74° and 78° inclinations, or between the 21-day and 22-day repeat periods.

References
ALSDORF, D.E., RODRIGUEZ, E. and LETTENMAIER, D.P., 2007, Measuring surface water from space, *Reviews of Geophysics*, **45**, RG2002, doi:10.1029/2006RG000197.

BIANCAMARIA, S., ANDREADIS, K., DURAND, M., CLARK, E., RODRIGUEZ, E., MOGNARD, N., ALSDORF D., LETTENMAIER, D. and OUDIN, Y., 2010, Preliminary characterization of SWOT hydrology error budget and global capabilities. *Journal of Selected Topics in Earth Observations and Remote Sensing*, **3**, pp. 6–19.

BIRKETT, C.M., 1995, The contribution of TOPEX/POSEIDON to the global monitoring of climatically sensitive lakes. *Journal of Geophysical Research*, **100**, pp. 25179–25204.

BIRKETT, C.M., 1998, Contribution of the TOPEX NASA radar altimeter to the global monitoring of large rivers and wetlands. *Water Resources Research*, **34**, pp. 1223–1239.

BIRKETT, C.M., MERTES, L.A.K., DUNNE, T., COSTA, M.H. and JASINSKI, M.J., 2002, Surface water dynamics in the Amazon Basin: Application of satellite radar altimetry. *Journal Geophysical Research*, **107**, D208059, doi:10.1029/2001JD000609.

CARPENTER, S.R., FISHER, S.G., GRIMM, N.B. and KITCHELL, J.F., 1992, Global change and freshwater ecosystems. *Annual Review of Ecology and Systematics*, **23**, pp. 119–139.

CRAPPER, P.F., 1980, Errors incurred in estimating an area of uniform land cover using Landsat. *Photogrammetric Engineering and Remote Sensing*, **46**, pp. 1295–1301.

DOWNING, J.A., PRAIRIE, Y.T., COLE, J.J., DUARTE, C.M., TRANVIK, L.J., STRIEGL, R.G., MCDOWELL, W.H., KORTELAINEN, P., CARACO, N.F., MELACK, J.M. and MIDDELBURG, J.J., 2006, The global abundance and size distribution of lakes, ponds, and impoundments. *Limnology and Oceanography*, **51**, pp. 2388–2397.

DURAND, M., ANDREADIS, K.M., ALSDORF, D.E., LETTENMAIER, D.P., MOLLER, D. and WILSON, M., 2008, Estimation of bathymetric depth and slope from data assimilation of swath altimetry into a hydrodynamic model. *Geophysical Research Letters*, **35**, L20401, doi:10.1029/2008GL034150.

HARDY, D.R., 1996, Climatic influences on streamflow and sediment flux into Lake C2, northern Ellesmere Island, Canada. *Journal of Paleolimnology*, **16**, pp. 133–149.

KIM, J.-W., LU, Z., LEE, H., SHUM, C.K., SWARZENSKI, C.M., DOYLE, T.W. and BAEK, S.-H., 2009, Integration analysis of PALSAR/Radarsat-1 InSAR and ENVISAT altimeter data for mapping of absolute water level changes in Louisiana wetlands. *Remote Sensing of Environment*, **113**, pp. 2356–2365.

KOURAEV, A.V., ZAKHAROVA, E.A., SAMAIN, O., MOGNARD, N.M. and CAZENAVE, A., 2004, Ob' river discharge from TOPEX/Poseidon satellite altimetry. *Remote Sensing of Environment*, **93**, pp. 238–245.

LEE, H., SHUM, C.K., YI, Y., IBARAKI, M., KIM, J.-W., BRAUN, A., KUO, C.-Y. and LU, Z., 2009, Louisiana wetland water level monitoring using retracked TOPEX/POSEIDON altimetry. *Marine Geodesy*, **32**, pp. 284–302.

LEHNER, B. and DÖLL, P., 2004, Development and validation of a global database of lakes, reservoirs and wetlands. *Journal of Hydrology*, **296**, pp. 1–22.

MEYBECK, M., 1995, Global distribution of lakes. In *Physics and Chemistry of Lakes*, A. Lerman, D.M. Imboden and J.R. Gat (Eds), pp. 1–35 (Berlin: Springer-Verlag).

MOLLER, D., RODRIGUEZ, E. and DURAND, M., 2008, Temporal decorrelation and topographic layover impact on Ka-band swath altimetry for surface water hydrology. In *Eos Transactions AGU*, **89**, Fall Meeting Supplement, Abstract H41B-0877.

MORRIS, C.S. and GILL, S.K., 1994, Evaluation of the TOPEX/POSEIDON altimeter system over the Great Lakes. *Journal of Geophysical Research*, **99**, pp. 24527–24539.

NATIONAL RESEARCH COUNCIL, 2007, *Earth Science and Applications from Space: National Imperatives for the Next Decade and Beyond* (Washington, DC: National Academies press).

PAPA, F., LEGRESY, B., MOGNARD, N., JOSBERGER, E.G. and REMY, F., 2002, Estimating terrestrial snow depth with the TOPEX/Poseidon altimeter and radiometer. *IEEE Transactions on Geoscience and Remote Sensing*, **40**, pp. 2162–2169.

PARKE, M.E., STEWART, R.H. and FARLESS, D.L., 1987, On the choice of orbits for an altimetric satellite to study ocean circulation and tides. *Journal of Geophysical Research*, **92**, pp. 11693–11707.

PAVELSKY, T.M. and SMITH, L.C., 2008, Remote sensing of hydrologic recharge in the Peace-Athabasca Delta, Canada. *Geophysical Research Letters*, **35**, L08403, doi:10.1029/2008GL033268.

PETERSON, B.J., HOLMES, R.M., MCCLELLAND, J.W., VÖRÖSMARTY, C.J., LAMMERS, R.B., SHIKLOMANOV, A.I., SHIKLAMANOV, I.A. and RAHMSTORF, S., 2002, Increasing river discharge to the Arctic ocean. *Science*, **298**, pp. 2171–2173.

SHENG, Y., 2008, Theoretical accuracy analysis of water storage change for the SWOT mission. In *International Workshop on Microwave Remote Sensing for Land Hydrology*, 20–22 October 2008, Oxnard, CA.

SMITH, L. and PAVELSKY, T., 2009, Remote sensing of volumetric storage changes in lakes. *Earth Surface Processes and Landforms*, **34**, pp. 1353–1358.

SMITH, L., SHENG, Y., MACDONALD, G.M. and HINZMAN, L.D., 2005, Disappearing Arctic lakes. *Science*, **308**, p. 1429.

WETZEL, R.G., 1992, Clean water: a fading resource. *Hydrobiologia*, **243/244**, pp. 21–30.